# Journal of Materials Chemistry A

Accepted Manuscript






ROYAL SOCIETY OF CHEMISTRY

www.rsc.org/materialsA

Journal Name

RSCPublishing

ARTICLE

# Anti-fluorite $Li_6CoO_4$ as an alternative lithium source for lithium ion capacitors: An experimental and first principles study

Cite this: DOI: 10.1039/x0xx00000x

Received 00th January 2012,
Accepted 00th January 2012

DOI: 10.1039/x0xx00000x

www.rsc.org/

Young-Geun Lim,[a,e,‡] Duho Kim,[b,‡] Jin-Myoung Lim,[b] Jeom-Soo Kim,[a,d] Ji-Sang Yu,[a] Young-Jun Kim,[a] Dongjin Byun,[e] Maenghyo Cho,[b] Kyeongjae Cho*[b,c] and Min-Sik Park*[a]

As a promising hybrid energy storage system, lithium ion capacitors (LICs) have been intensively investigated regarding their practical use in various applications, ranging from portable electronics to grid support. The asymmetric LIC offers high-energy and high-power densities compared with conventional energy storage systems such as electrochemical double-layer capacitors (EDLCs) and lithium ion batteries (LIBs). To enable proper operation of the LIC, the negative electrode should be pre-lithiated prior to cell operation, which is regarded as a key technology for developing self-sustainable LICs. In this work, we have demonstrated the potential use of $Li_6CoO_4$ as an alternative lithium source to metallic lithium. A large amount of $Li^+$ can be electrochemically extracted from the structure incorporated into the positive electrode via a highly irreversible process. Most of the extracted $Li^+$ is available for pre-lithiation of the negative electrode during the first charge. This intriguing electrochemical behaviour of $Li_6CoO_4$ is suitable for providing sufficient $Li^+$ to the negative electrode. To obtain a fundamental understanding of this system, the electrochemical behaviour and structural stability of $Li_6CoO_4$ is thoroughly investigated by means of electrochemical experiments and theoretical validation based on first principles calculations.

## Introduction

Concerns have been raised about hybrid energy storage systems due to the growing demand for suitable power sources in various applications for peak assist power and load leveling of renewable energy supplies.[1-6] Such applications have different specific requirements for energy and power densities.[7] Among various candidates for multi-purpose energy storage systems,[5,7-9] lithium ion capacitors (LICs) have aroused a great interest due to their ability to expand the energy storage market owing to their controllable electrochemical characteristics and excellent durability.[10-12]

The LIC is one of the hybrid capacitors that combines the strengths of an electrochemical double-layer capacitor (EDLC) and a lithium ion battery (LIB), and offers high power and energy. Due to the synergy of both conventional energy storage systems, the LIC is able to achieve more than three times higher energy density than conventional EDLC, while also featuring superior power characteristics compared with the LIB.[2,10,11,13,14] The hybrid cell configuration of the LIC allows: i) fast charging, ii) high operating voltages, and iii) excellent durability. On the basis of those premises, it is expected to become an advanced energy storage system that is widely applicable in the currently opened new markets. In particular, the consumption value of LICs in wind power generation is forecast to reach over $150 million in 2021.[14-17]

The most important technical issue involved in developing high-energy LICs is to develop an efficient means of pre-lithiation of the negative electrode (NE) to allow for proper cell operation. In this regard, we recently suggested a new $Li^+$ pre-doping method, through the integration of highly irreversible transition metal oxides such as $Li_2MoO_3$ and $Li_5FeO_4$ in the positive electrode (PE) of the LIC, as alternative $Li^+$ sources to the auxiliary metallic Li electrode.[18-20] The proposed cell configuration allows a higher $Li^+$ doping efficiency (> 90%) and better durability compared with the conventional LIC using metallic Li. Note that by removing metallic Li from the cell, the benefits of additional volumetric energy density of the cell as well as securing the improvement of its safety, can be attained.

An important qualification of the $Li^+$ source materials to be integrated in the PE is a high irreversibility toward $Li^+$ insertion and extraction, mainly responsible for sufficient $Li^+$ pre-doping into the NE. However, $Li_2MoO_3$ and $Li_5FeO_4$ suffer from requiring a high voltage operation (> 4.7 V vs. $Li/Li^+$) to provide sufficient $Li^+$ to the NE, which possibly causes the

inevitable side reactions associated with electrolyte decomposition as well as performance degradation mainly caused by pore clogging of activated carbon due to the high voltage operation. More efforts are still required, therefore, to find new alternative $Li^+$ sources in the development of advanced LICs.

As part of an effort to find new materials capable of providing a large amount of irreversible $Li^+$, our priority has been to consider various Li-rich materials. Among them, $Li_6CoO_4$, which has an anti-fluorite structure, is a promising candidate because of its high theoretical capacity (>900 mAh $g^{-1}$) and poor reversibility in the first cycle.[21] The distinct electrochemical behaviour of $Li_6CoO_4$ is definitely an attractive feature as an alternative $Li^+$ source in our proposed concept. A huge amount of $Li^+$ can be extracted from $Li_6CoO_4$, but most of the extracted $Li^+$ does not reversibly insert into the structure due to its unique crystal structure. Even though it has not been successfully deployed as a cathode material for practical use in LIBs because of its high irreversibility, another possibility for the use of $Li_6CoO_4$ has been verified as a functional additive for compensating the low coulombic efficiency of Si-based anode materials.[22] The integration of highly irreversible $Li_6CoO_4$ into the cathodes was effective in increasing the practical capacity of the LIB, by minimizing the capacity loss originating from the large initial irreversible capacity of Si-based anode materials. This positive effect of $Li_6CoO_4$ has been evaluated in LIB applications, but fundamental studies on the structural and electrochemical properties of $Li_6CoO_4$ have not been fully conducted yet.

On the other hand, $Li_6CoO_4$ also has great potential as a promising $Li^+$ source compared with other candidates such as $Li_2MoO_3$ and $Li_5FeO_4$. A total 6 mol of $Li^+$ are occupied in the given structure and about 4 mol of $Li^+$ can be electrochemically extracted from the structure with a cut-off voltage of 4.3 V vs. $Li/Li^+$, which makes this extremely valuable as an alternative $Li^+$ source. The $Li^+$ pre-doping can be carried out with a relatively smaller amount of $Li_6CoO_4$ owing to its high initial charge capacity and irreversibility. More importantly, sufficient $Li^+$ can be provided by incorporation of $Li_6CoO_4$ with a low cut-off voltage (below 4.3 V vs. $Li/Li^+$), while $Li_2MoO_3$ and $Li_5FeO_4$ suffer from undesirable side reactions associated with electrolyte decomposition at high voltage operation (over 4.7 V vs. $Li/Li^+$).[18-20] Therefore, it should be emphasized that the use of $Li_6CoO_4$ can effectively prevent side reactions originating from electrolyte decomposition, generally caused by high voltage operation above 4.3 V vs. $Li/Li^+$.

Herein, we examine the potential use of $Li_6CoO_4$ as a promising $Li^+$ source to allow efficient $Li^+$ pre-doping in the LIC. To demonstrate convincingly the key advantages of using $Li_6CoO_4$, we investigated its capability as an alternative $Li^+$ source in the LICs based on various experiments combined with theoretical calculations. Our findings also promote further understanding of the structural and electrochemical properties of $Li_6CoO_4$, to consolidate the proposed $Li^+$ pre-doing method for enabling greater energy storage and efficiency of LICs.

## Experimental

### Structural Characterizations

To synthesize single-phase $Li_6CoO_4$ powder, stoichiometric amounts of $Li_2O$ (>97%, Aldrich) and CoO (>99%, Aldrich) powders were homogeneously mixed at a molar ratio of 3:1 using a ball mill for 12 h. The mixture was heated at 700 °C for 12 h in a sealed tube furnace under an Ar atmosphere. To prevent contact with moisture, the collected power was handled carefully in a dry room. The structure of the final product was determined using an X-ray diffractometer (XRD, PANalytical, Emyrean) equipped with a 3D pixel semiconductor detector and Cu-K$\alpha$ radiation ($\lambda$ = 1.54056 Å). The in situ XRD analysis was carried out using a homemade test cell. The cell was charged and discharged at a constant current density of 0.05 C (32 mA $g^{-1}$) in the voltage range of 2.5 to 4.3 V (vs. $Li/Li^+$) and the XRD patterns were collected at various state-of-charge (SOC) states during the first cycle. The chemical composition of as-prepared $Li_6CoO_4$ powder was confirmed by inductively coupled plasma mass spectroscopy (ICP-MS, Bruker Aurora M90) analysis. Field emission scanning electron microscopy (FESEM, JEOL JSM-7000F) and high-resolution transmission electron microscopy (HRTEM, JEOL ARM-200F) were employed to examine the morphology and microstructure of the final product. In addition, the chemical states of the final product and electrodes collected at various SOC states during the first cycle were identified by X-ray photoelectron spectroscopy (XPS) using a sigma probe spectrometer (Thermo Scientific). For ex-situ XPS analyses, the cells were carefully disassembled in Ar-filled glove box and the collected electrodes were washed with dimethyl carbonate (DMC) solution to remove residual salts. After drying, the electrodes transferred into another Ar-filled glove box attached on XPS using a portable airtight container.

### Electrochemical Measurements

The PE, composed of activated carbon (80.9 wt% and 74.8 wt%, MSP-20, Kansai Coke and Chemicals) and $Li_6CoO_4$ (11.1 wt% and 17.2 wt% for 60% doping and 100% doping of practical NE capacity, respectively), was prepared by coating a slurry, containing the active materials (92 wt%) and PVDF (polyvinylidene difluoride, 8 wt%) binder, dissolved in an NMP (*N*-methyl-2-pyrolidinone) solution, on Al mesh. The NE was prepared by coating a slurry, containing hard carbon (80 wt%, Kureha Corporation), a conducting agent (super-P, 10 wt%), and PVDF binder (10 wt%), on Cu mesh. The amount of $Li_6CoO_4$ in the PE was decided based on the corresponding NE capacity (0.404 mAh; 60% doping level, 0.673 mAh; 100% doping level) and the specific capacity of $Li_6CoO_4$ (630 mAh $g^{-1}$) with a cut-off voltage of 4.3 V vs. $Li/Li^+$. The loading level and density of the PE were fixed at 6.4 mg $cm^{-2}$ and 0.5 g $cc^{-1}$ for 60% doping, and 6.9 mg $cm^{-2}$ and 0.5 g $cc^{-1}$ for 100% doping (Table S2). As for the NE, the loading level and density were 2.2 mg $cm^{-2}$ and 0.8 g $cm^3$, respectively. The beaker-type half cells and full cells were carefully assembled in a dry room

to evaluate their electrochemical performance. In order to examine $Li^+$ pre-doping behaviour of LIC full cell, 4-electrode cell composed of PE, NE, and two Li electrodes as reference electrodes was designed as described in Fig. S3. The PE and NE were punched into disks, with diameters of 12 and 14 mm, respectively, and 8 mL of electrolyte was added into each cell. A porous polyethylene (PE) membrane was used as the separator, and 1.3 M $LiPF_6$ dissolved in ethylene carbonate (EC) / dimethyl carbonate (DMC) (3:7 v/v, PANAX ETEC Co. Ltd) was used as the electrolyte. All electrochemical data were obtained at room temperature.

### DFT Simulations

All calculations were conducted with density functional theory (DFT) along with +U using the Vienna Ab Initio Simulation Package (VASP). Core electrons were represented by the projector augmented wave method with pseudo-potentials. For accurate $Li^+$, the pseudo-potentials cover all three electrons of Li (Li_sv) with the 2*s* states being treated as valence states, and the general potentials of Co and O are used. The local density approximation (LDA+U) was used for the exchange-correlation functional for the spin-polarized calculations. Based on the obtained electrochemical data, the U parameter (9.9 eV) was used here for the *3d* levels of Co because no experimental gap was observed for $Li_6CoO_4$. In this work, the general computational parameters included a plane-wave cut-off energy of 600 eV, expanded by the use of wave functions and 2×2×2 k-point sampling, based on the Monkhorst-Pack method. The atomic configurations and cell parameters were fully optimized in order to calculate the total internal energy in the first calculation. During de-lithiation ($Li^+$ extraction), the cell volume was fixed; however, the ions involved in the cell were relaxed.

## Results and discussion

Single-phase $Li_6CoO_4$ powder was successfully synthesized by a conventional solid state reaction by heating stoichiometric amounts of $Li_2O$ and CoO precursors under optimized conditions. Fig. 1a and 1b show the field-emission scanning electron microscopy (FESEM) and transmission electronic microscopy (TEM) images, respectively, indicating that the irregularly shaped $Li_6CoO_4$ powders have an average particle size of about 30 μm (Fig. S4). We examine the microstructure of $Li_6CoO_4$ further by high-resolution TEM, as shown in Fig. 1c. Observation by HRTEM, combined with selected area diffraction pattern (SADP), confirmed the fine microstructure of $Li_6CoO_4$ with tetragonal symmetry and showed that the *d*-spacing of the zone axis [101] was approximately 3.8 Å. Fig. 1d shows the powder X-ray diffraction (XRD) pattern of the as-prepared $Li_6CoO_4$ powders. All reflections are indexed to tetragonal $Li_6CoO_4$ with an anti-fluorite structure (JCPDF #38-1140), which belongs to a space group of P42/*nmc*. After refinement, the lattice parameters of $Li_6CoO_4$ were estimated to be $a = b = 6.539(8)$ Å and $c = 4.648(0)$ Å, which were in good agreement with the previously reported values.[23] In addition,

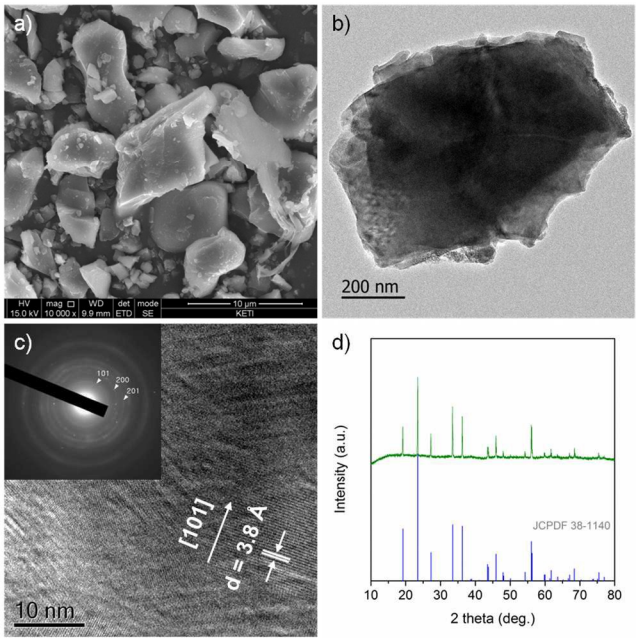


**Fig. 1** (a) Field-emission scanning electron microscopy (FESEM) image of $Li_6CoO_4$, (b) Transmission electron microscopy (TEM) image of $Li_6CoO_4$, (c) High-resolution TEM image of $Li_6CoO_4$, combined with selected area electron diffraction pattern (SADP) in the inset, and (d) Powder X-ray diffraction (XRD) pattern of $Li_6CoO_4$, together with a reference pattern (JCPDF 38-1140).

we could not find any evidence of impurities or secondary phase formation. Furthermore, the chemical composition of $Li_6CoO_4$ was also confirmed by inductively coupled plasma (ICP) analysis. According to the result (Table S3), the ratio of Li to Co was estimated to be 6.09, indicating that some residual Li would have remained on the surface. Based on the various structural analyses, we believe that single-phase $Li_6CoO_4$ powders were successfully synthesized without undesirable oxygen deficiency.

Fig. 2a shows galvanostatic charge ($Li^+$ extraction) and discharge ($Li^+$ insertion) profiles of $Li_6CoO_4$ combined with the corresponding in situ XRD patterns obtained at the first cycle. Note that $Li^+$ can be extracted from the structure with two distinctive plateau regions at around 3.5 and 3.8 V vs. $Li/Li^+$, during the initial charging to 4.3 V vs. $Li/Li^+$. At a subsequent discharge to 2.0 V vs. $Li/Li^+$, the extracted $Li^+$ does not reversibly insert into its de-lithiated structure ($Li_{6-x}CoO_4$). As a result, a very poor initial coulombic efficiency of 1.14 % was attained at the first cycle. To be more specific, the charge capacity responsible for $Li^+$ extraction was estimated to be 630.2 mAh $g^{-1}$ (about 3.75 mol of $Li^+$ extraction) and only 7.2 mAh $g^{-1}$ for $Li^+$ insertion at the first cycle, which is also evidently confirmed in ex-situ ICP results obtained at various state-of-charge (SOC) as summarized in Table S4. The corresponding in situ XRD patterns (Fig. 2b) collected at various SOC states also support the high irreversibility of $Li_6CoO_4$ as the appropriate structural viewpoint. The XRD pattern of the $Li_6CoO_4$ electrode, collected at open-circuit voltage (OCV), was identical to that of the powder XRD

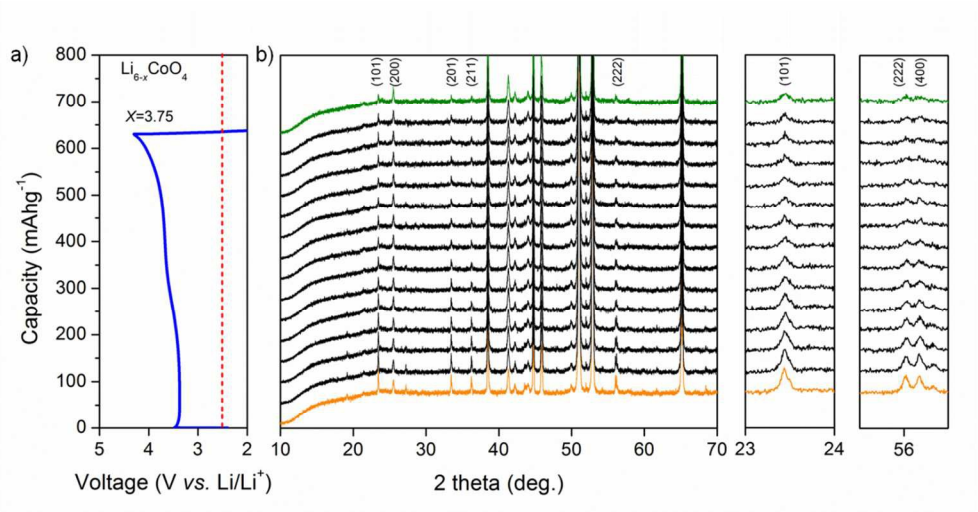


**Fig. 2** (a) Galvanostatic charge ($Li^+$ extraction) and discharge ($Li^+$ insertion) profiles of $Li_6CoO_4$ in a voltage range of 2.0 to 4.3 V vs. $Li/Li^+$ with a constant current density of 0.05 C (32 mA $g^{-1}$) and (b) corresponding in situ X-ray diffraction (XRD) patterns of $Li_{6-x}CoO_4$ during the first charge. Changes in (101), (222), and (400) peaks are enlarged on the right.

pattern, except for some diffractions arising from the Al current collector and the Be window. Along with $Li^+$ extraction, the intensity of the (101), (222), and (400) peaks of $Li_6CoO_4$ were gradually reduced without significant peak shifts. These $Li_6CoO_4$ peaks remained unchanged during the subsequent $Li^+$ insertion, revealing that the extracted $Li^+$ could not be electrochemically inserted into the host structure again.

For further inspection on the structural change of $Li_6CoO_4$ during $Li^+$ extraction, we conducted by ex situ X-ray photoelectron spectroscopy (XPS) analysis, as shown in Fig. 3. We focused on the change in the valence state of Co, which governed $Li^+$ extraction and insertion into the $Li_6CoO_4$ structure. The Co $2p_{3/2}$ spectra, collected from various SOC states, were carefully fitted to the C 1s spectra at 284.6 eV (Fig. 3a). As expected, a dominant peak was found at 779.8 eV, corresponding to $Co^{2+}$ before the $Li^+$ extraction from the structure as shown in Fig. 3b. When $Li^+$ extraction proceeded until $x$ = 1.0 in the $Li_{6-x}CoO_4$, $Co^{3+}$ peak at 780.4 eV was dominantly observed, indicating that the redox reaction of $Co^{2+}/Co^{3+}$ is mainly responsible for the initial $Li^+$ extraction. After further $Li^+$ extraction proceeded up to $x$ = 2.0, the $Co^{3+}$ peak was decreased while the growth of $Co^{4+}$ peak at 781.4 eV was noticeable, responsible for $Co^{3+}/Co^{4+}$ redox reaction. Beyond $x$ = 2.0, we found that the $Co^{4+}$ could not be further oxidized as evidenced by the Co $2p_{3/2}$ spectrum at the end of the charge ($x$ = 3.75). In order to identify an exact $Li^+$ extraction mechanism of $Li_6CoO_4$, we also studied changes in the O 1s spectra. Fig. 3c shows O 1s spectra collected at different SOC states. There was no noticeable change in the collected spectra due to $Li^+$ extraction until $x$ = 2.0. Interestingly, a significant peak shift, from 529.3 to 529.8 eV, was obvious at the end of the charge ($x$ = 3.75). It seems that structural change may be induced by further $Li^+$ extraction from the structure for values above $x$ = 2.0. For practical use of $Li_6CoO_4$, there is a string need for further theoretical study on the $Li^+$ extraction mechanism and structural stability of $Li_{6-x}CoO_4$.

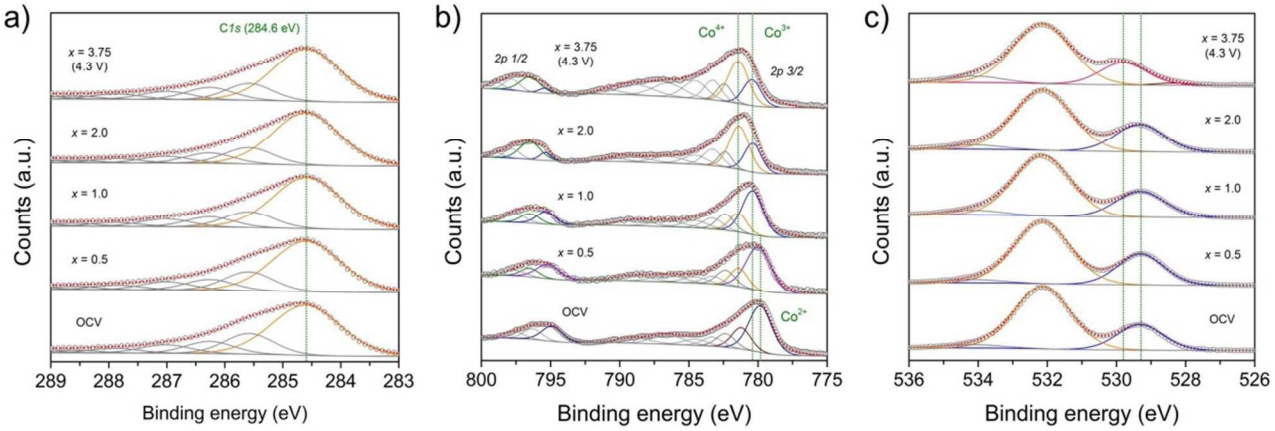


**Fig. 3** Ex situ X-ray photoelectron spectroscopy (XPS) spectra of (a) C 1s, (b) Co 2p, and (c) O 1s at different state of charge (SOC) states; $x$ = 0 (OCV), 0.5, 1.0, 2.0, and 3.75 (4.3 V vs. $Li/Li^+$ cut-off) of $Li_{6-x}CoO_4$.

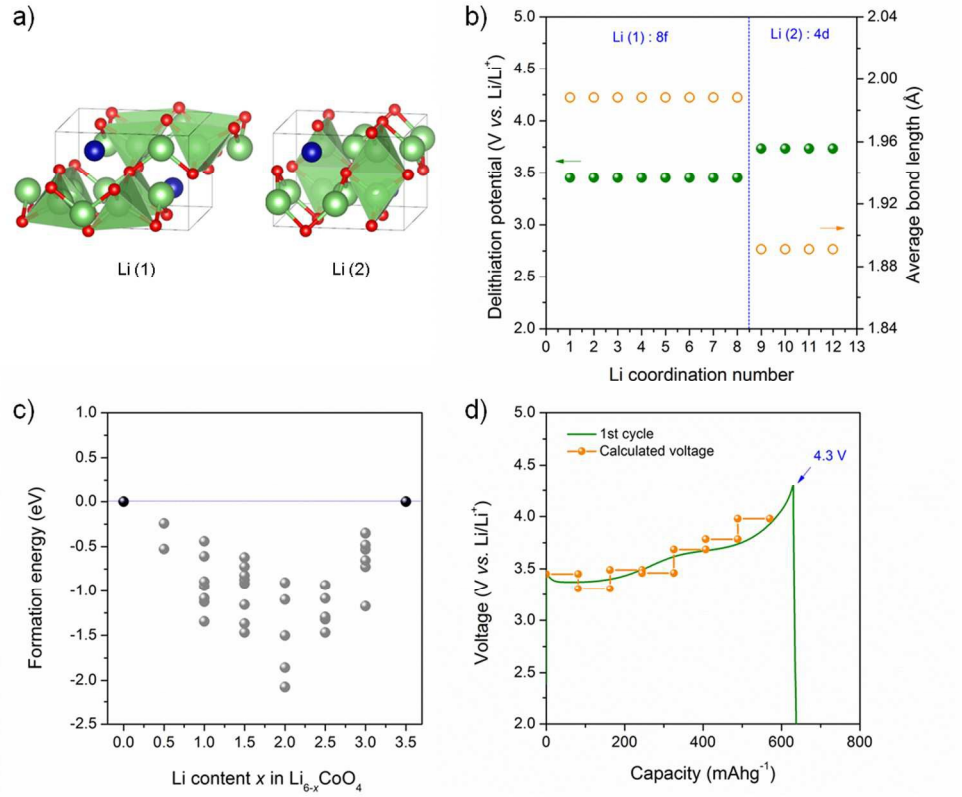


**Fig. 4** (a) Crystal structures of anti-fluorite $Li_6CoO_4$ with a tetragonal symmetry (space group: P42/*nmc*), in which Li(1), Li(2), Co, and O are occupied in *8f*, *4d*, *2a* and *8g* sites, respectively, in terms of the Wyckoff position, (b) De-lithiation potentials of $Li^+$ in Li(1) and Li(2) sites and average bond length of $Li^+$ in Li(1) and Li(2) sites, (c) Relative formation energy of $Li_{6-x}CoO_4$ with respect to Li content, and (d) Comparison of the calculated de-lithiation potentials and galvanostatic charge curve of $Li_{6-x}CoO_4$ at the first charge.

For the theoretical study, a tetragonal $Li_6CoO_4$ structure (space group: P42/*nmc*) was modeled as described in Fig. 4a, in which Li(1), Li(2), Co, and O occupy the *8f*, *4d*, *2a*, and *8g* sites, respectively, in terms of the Wyckoff positions.[23] Our initial concern regarded the distinct de-lithiation potentials of $Li_6CoO_4$, observed at 3.5 and 3.8 V vs. $Li/Li^+$ in the electrochemical experiments (Fig. S5). The average de-lithiation potentials, $\bar{E}$, were obtained from total energy values calculated by density functional theory (DFT), based on Eqn. 1.[24,25] In this calculation, the Gibbs free energy ($\Delta G$) term was approximated by the total internal energy ($\Delta E$), and small changes in entropy ($T\Delta S$) and volume ($P\Delta V$) were not considered. The average de-lithiation potential of $Li_6CoO_4$ can be accordingly found from

$$\overline{V} = \frac{E_{tot}[Li_{x_2}CoO_4] - E_{tot}[Li_{x_1}CoO_4] - (x_2 - x_1)E[Li]}{x_2 - x_1} \quad (1)$$

where $x_2$ is the number of $Li^+$ in the fully lithiated state ($Li_6CoO_4$), $x_1$ is the number of $Li^+$ located in intermediate de-lithiated state ($Li_{6-x}CoO_4$), and $E_{tot}$ expresses the total internal energy of the structure. $E[Li]$ is the chemical potential of metallic Li in the *bcc* structure.

The de-lithiation potential was studied from two perspectives for different Li sites, known as Li(1) and Li(2), as described in Fig. 4b. The calculated de-lithiation potentials of $Li^+$ in Li(1) and Li(2) sites were approximately 3.5 and 3.8 V vs. $Li/Li^+$, respectively, which were in good agreement with our experimental results. Note that the de-lithiation potentials are strongly dependent on the positions of $Li^+$ in the $Li_6CoO_4$ structure, which can be further understood from the changes in bond lengths (between Li and O) and the average net charges (Li and O), which affect the local Coulomb interaction energy in the $LiO_4$ tetrahedral geometry. The average bond length between Li and O was calculated to be 1.98 and 1.89 Å for Li(1) and Li(2) sites, respectively, as described in Fig. 4b. This indicates that the bonding strength of the Li(2) site is stronger than that of the Li(1) site in the relaxed $Li_6CoO_4$ structure, which directly affects the Li site energy surrounded by O. Thus, the Li(2) site has a higher de-lithiation potential compared with the Li(1) site. We also confirmed the presence of different average net charges of $Li^+$ positioned in the Li(1) and Li(2) sites, from the Bader charges analysis on the relaxed $Li_6CoO_4$ structure; however, no noticeable difference was found in the average net charges of O in all the positions in the structure (Fig. S6a). Based on the calculations for average bond lengths and net charges, attractive pair electrostatic interaction was also

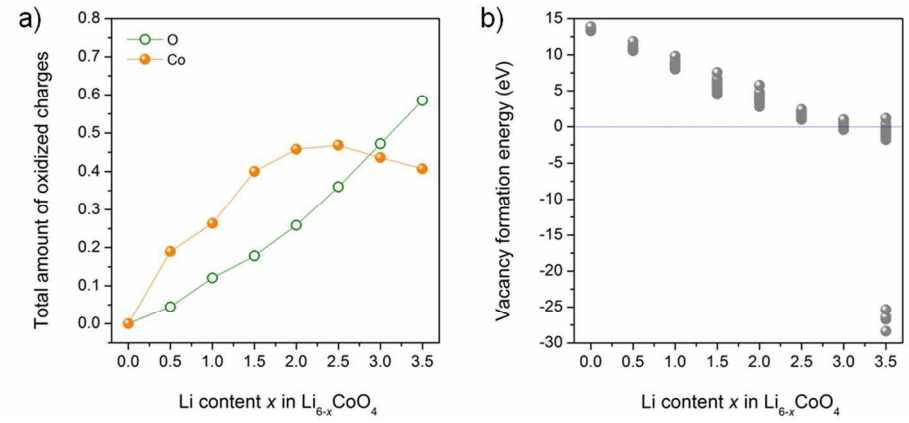


**Fig. 5** (a) Total amount of electrons formed by oxidation of Co and O, and (b) O vacancy formation energy of $Li_{6-x}CoO_4$ with respect to Li contents ($0 \le x < 4.0$) during the first charge.

evaluated by taking into account the ratio $q_i q_j / r_{ij}$ (Eqn. S2), the value of which depends on the type of Li site (Fig. S6b).[25] The higher negative value corresponds to the higher electrochemical potential and the lower negative value corresponds to the lower electrochemical potential. Therefore, the Li(2) site forms a relatively strong bond with O compared with the Li(1) site, which supports the idea that the two different plateaus originate from the local environment of different Li sites.

The relative formation energy ($E^r_f$) of $Li_{6-x}CoO_4$ with respect to the Li content was calculated to investigate the structural stability of the tetragonal structure associated with $Li^+$ extraction (Eqn. S3).[26,27] The formation energy was calculated for the practically usable composition of $Li_{6-x}CoO_4$ ranging from $x = 0$ to 4.0. Fig. 4c shows a comparison of the formation energy of possible $Li^+$ configurations in each de-lithiated form of $Li_{6-x}CoO_4$. The structure of $Li_{6-x}CoO_4$ in the range of $0 \le x < 4.0$ would be thermodynamically stable, as evidenced by the in situ XRD data and formation energy calculations during the first charge that were mentioned above. By taking into account a sequential de-lithiation process (Fig. 4d), the theoretical voltages are considered to correspond with the ground state energy at each Li concentration. According to the formation energy calculation using Eqn. S4, the de-lithiated $Li_{6-x}CoO_4$ structure ($x < 4.0$) are more unstable compared with the original structure $Li_6CoO_4$ ($x = 0$) and tend to become increasingly unstable with increasing $Li^+$ extraction for the crystal structure composed of the tetrahedral frameworks (Co-O), shown in Fig. S7. However, the formation energy became thermodynamically stable when further $Li^+$ was extracted to produce $Li_{6-x}CoO_4$ ($x = 4.0$). This may be caused by structural collapse, which is responsible for unexpected turning out of the total energy. We investigated the electronic structures of $Li_{6-x}CoO_4$ to improve our understanding of this phenomenon. Fig. S8 shows O 2p partial density of states (PDOS) in $Li_{6-x}CoO_4$ with different $Li^+$ contents, and presents the oxidation behaviours of O. There are no noticeable electrons around 0 to 4.0 eV in the fully lithiated state ($x = 0$), while a noticeable amount of electrons was found within the same range in the unoccupied state of the partially de-lithiated state ($x < 4.0$). It should be noted that a loss of electrons from O occurred in the $Li_{6-x}CoO_4$ structure and the total amount of the electrons generated by O oxidation increased during the $Li^+$ extraction, leading to an unstable environment of the tetrahedral geometries (Li-O and Co-O). Furthermore, we investigated the average net charges of O and Co to demonstrate their oxidation tendency during $Li^+$ extraction. Fig. 5a presents the total amount of oxidized charge, based on the calculated average net charges of O and Co in $Li_{6-x}CoO_4$, along with the $Li^+$ removal. We found that the charge transfer from O consistently increased as $Li^+$ extraction proceeded, however the oxidation behaviour of Co was quite different. The initial oxidation state of Co in the $Li_6CoO_4$ was $Co^{2+}$, as evidenced by the XPS spectra. During the de-lithiation process, $Co^{2+}$ could be oxidized to $Co^{3+}$ until 1 mol of $Li^+$ was extracted ($x = 1.0$); then further oxidation to $Co^{4+}$ was observed until $x = 2.0$. However, it would be difficult to withdraw more electrons beyond $x = 2.0$ from the host structure because $Co^{4+}$ cannot be further oxidized to $Co^{5+}$ due to its stable electronic structure. Thus, continuous loss of electrons from O occurred by further $Li^+$ extraction ($x \ge 2.0$), which would increase the possibility of the structural instability of $Li_6CoO_4$. The possibility of oxygen evolution can be explained using the formation energy of the O vacancies ($E_v$) (Eqn. 2), expressed as

$$E_v = E_{tot}\left[Li_{6-x_1}CoO_{4-x_2}\right] - E_{tot}\left[Li_{6-x_1}CoO_4\right] + \frac{1}{2}x_2 E[O_2] \quad (2)$$

where $x_1$ is the number of partially extracted $Li^+$, $x_2$ is the number of extracted O atoms for formation oxygen gas, $E_{tot}$ refers to the total energy of the structures and $E[O_2]$ is the chemical potential of $O_2$. Fig. 5b shows the O vacancy formation energy with respect to Li content in $Li_{6-x}CoO_4$. Note that the structures including oxygen vacancies showed positive vacancy formation energies below $x = 3.5$, indicating the thermodynamic instability of the vacancies. However, when $x > 3.5$, the vacancy formation energies become negative, which implies that the oxygen defected structures are relatively more stable.

These thermodynamic results are also reflected in the total amount of oxidized electrons, in terms of O and Co, beyond $x$ = 3.5 (Fig. 5b). The theoretical findings suggest that less than 3.5 mol of $Li^+$ can be extracted from $Li_6CoO_4$ without significant structural degradation, mainly associated with $O_2$ evolution. The $Li^+$ extraction from $Li_6CoO_4$ is governed by oxidation from

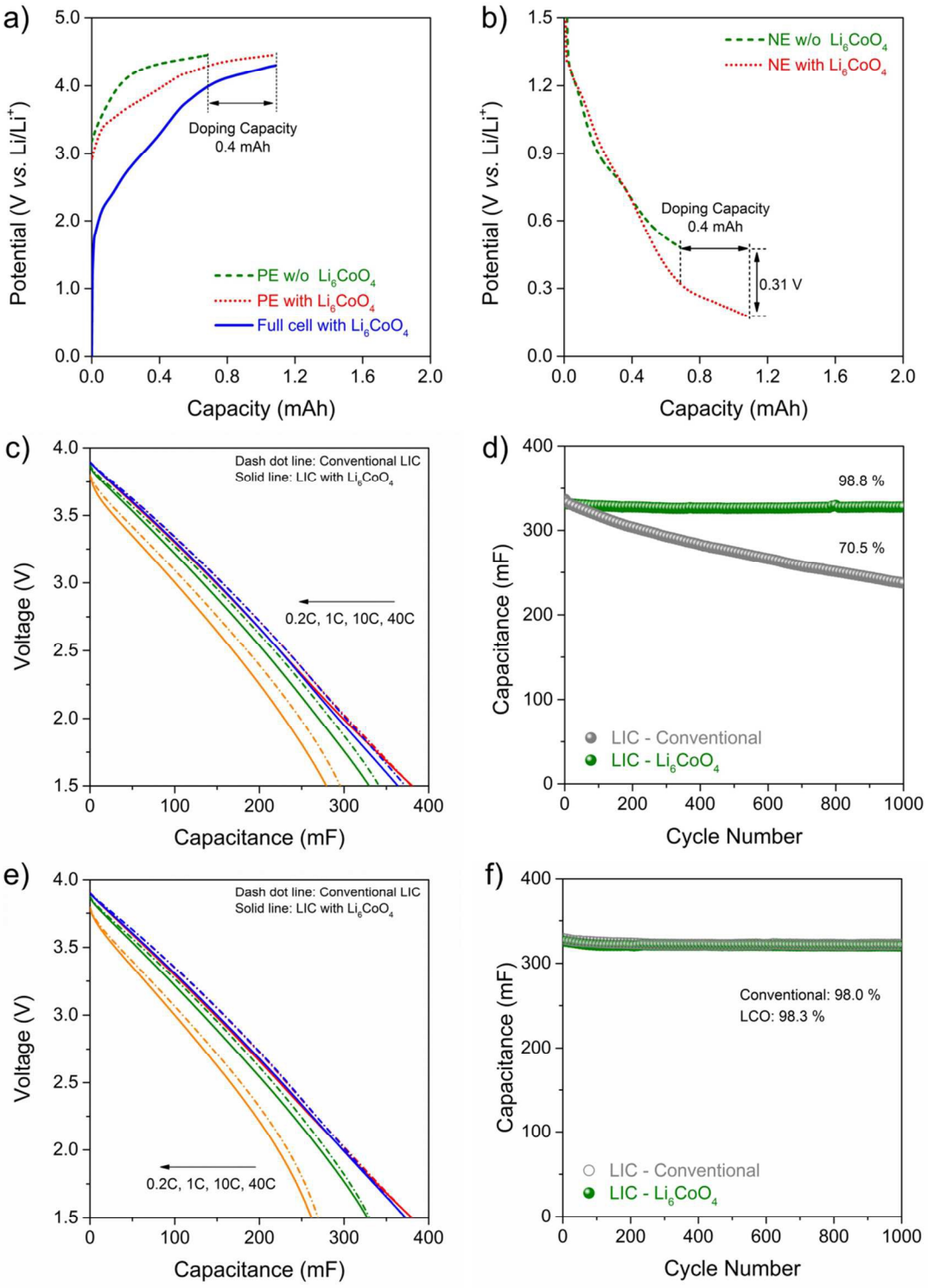


**Fig. 6** $Li^+$ pre-doping profiles (60% doping of practical NE capacity) of a LIC full cell with $Li_6CoO_4$ (11.1 wt%) as an alternative $Li^+$ source; corresponding voltage profiles of (a) the PE and (b) the NE during the first charge to 4.3 V vs. Li/$Li^+$. (c) Rate capability of the LIC full-cell with $Li_6CoO_4$ (60% doping) in a voltage range of 1.5 to 4.1 V at different current densities of 0.2, 1.0, 10, 20 C (1 C = 85 mA $g^{-1}$), and (d) Cycle performance of the LIC full cell with $Li_6CoO_4$ in a voltage range of 1.5 to 4.1 V at a constant current densities of 10 C. (e) Rate capability of the LIC full-cell with $Li_6CoO_4$ (100% doping), and (f) Cycle performance of the LIC full-cell with $Li_6CoO_4$ under the same experimental condition.

$Co^{2+}$ to $Co^{4+}$ until $x$ = 2.0 in the given structure, but the oxidation of O is mainly responsible for further $Li^+$ extraction ( $x \geq 2.0$).

Therefore, the available range of $Li^+$ in $Li_{6-x}CoO_4$ is below 3.5 mol for practical use in LIC of this alternative $Li^+$ source. To demonstrate this limit, we conducted an overcharging test to support our calculation result (Fig. S9). When $Li_6CoO_4$ was overcharged to 4.5 V vs. $Li/Li^+$ ($x$ = 4.0), an abnormal voltage profile was observed, which was associated with the structural collapse accompanied with $O_2$ evolution as found by DFT simulations.

$Li_6CoO_4$ has many advantages over the other candidates such as $Li_2MoO_3$ and $Li_5FeO_4$, which has been previously reported as alternative $Li^+$ sources for LICs.[18,19] $Li_6CoO_4$ allows efficient $Li^+$ pre-doping with a smaller amount, as well as a lower initial charging voltage than other candidates, which are beneficial for further improvement of energy density and safety. By reducing the amount of $Li_6CoO_4$, power loss that may possibly be induced by its poor electric conduction can be minimized. More importantly, electrolyte decomposition due to side reactions at high operating voltage (> 4.3 V vs. $Li/Li^+$) can be effectively prevented by applying a cut-off voltage below 4.3 V *vs.* $Li/Li^+$. The potential use of $Li_6CoO_4$ was examined for pre-lithiation of NE in LICs. Based on the electrochemical behavior of $Li_6CoO_4$, we designed a PE composed of activated carbon (80.9 wt) and $Li_6CoO_4$ (11.1 wt%), which can provide $Li^+$ for up to 60% of the NE total capacity (0.404 mAh). The 60% $Li^+$ pre-doping of a LIC full cell with $Li_6CoO_4$ in the PE was conducted by electrochemical charging to 4.3 V vs. $Li/Li^+$, and corresponding voltage profiles are presented in Fig. 6. For comparison, a LIC full cell without $Li_6CoO_4$ was also tested under the same conditions. From a voltage profile of the PE (Fig. 6a), a noticeable difference in the voltage profile of PE was observed during the first charge for $Li^+$ pre-doping. The PE containing $Li_6CoO_4$ exhibits two plateaus at 3.5 and 3.8 V vs. $Li/Li^+$, induced by $Li^+$ extraction from the integrated $Li_6CoO_4$ with a capacity of 0.404 mAh, which matched our design capacity. Fig. 6b shows a corresponding NE profile in which most of extracted $Li^+$ was efficiently delivered into the NE with the same capacity of 0.404 mAh. The end voltage of the NE in the LIC with $Li_6CoO_4$ was measured to be 0.18 V, which is 0.31 V lower than that of LIC without $Li_6CoO_4$ after the initial charging for $Li^+$ pre-doping. In addition, variation of $Li^+$ concentration in electrolyte was not significant before and after $Li^+$ pre-doping process (Table S5 in ESI), and surface oxidation state of the NE is not much different with that of NE in conventional (Fig. S10). Consequently, we confirmed that efficient $Li^+$ pre-doping of the NE could be achieved by the simple addition of $Li_6CoO_4$ into the PE.

After $Li^+$ pre-doping, electrochemical performance of the LIC full cell with $Li_6CoO_4$ was evaluated to examine its feasibility. Fig. 6c shows the rate-capability of the LIC full cell containing $Li_6CoO_4$ as an alternative $Li^+$ source compared with a conventional LIC with metallic Li. The discharge capacity of the LIC with $Li_6CoO_4$ was identical to that of conventional LIC at a low current density of 0.2 C (17 mA $g^{-1}$). However, at higher current densities, the capacities delivered by the LIC with $Li_6CoO_4$ were slightly lower than those of conventional LIC. This may be caused by the integration microscale $Li_6CoO_4$ into the PE, which induces a large overpotential at high currents (Fig. S11). We believe that this could be overcome by reducing the particle size of the $Li_6CoO_4$ or by introducing a conducting coating layer on its surface. To evaluate the cycle performance of the LIC full cell with $Li_6CoO_4$, the cell was cycled in a voltage range of 1.5 to 4.1 V at a constant current density of 10 C (850 mA $g^{-1}$). As shown in Fig. 6d, the LIC with $Li_6CoO_4$ showed an outstanding cycle performance during 1000 cycles. While the conventional LIC exhibited capacity retention of 70.5 % at the 1000th cycle, the LIC with $Li_6CoO_4$ maintained about 98.8 % of its initial capacity even after 1000 cycles. This excellent cycle performance is mainly attributed to the incorporation of $Li_6CoO_4$ instead of metallic Li because spontaneous $Li^+$ depletion could be minimized in the proposed LIC during the cycles (Fig. S12). This occurs because

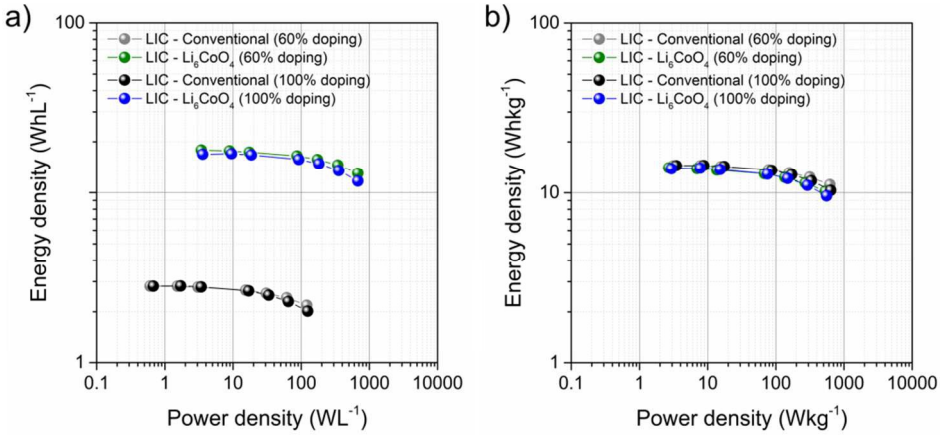


**Fig. 7** Fig. 7 Ragone plots of LIC full cells, containing $Li_6CoO_4$ as an alternative $Li^+$ source, compared with the conventional LIC, pre-lithiated with metallic Li: (a) volumetric energy and power densities, and (b) gravimetric energy and power densities. The weight and volume of electrolyte and exterior materials of LIC full cell was excluded in the calculation (see more detailed information in ESI).

undesirable Li deposition on the surface of NE, which is possibly induced by the conventional $Li^+$ pre-doping method can be prevented by incorporating $Li_6CoO_4$ as an alternative $Li^+$ source. Furthermore, the electrochemical performance of LIC, in particular employing hard carbon NEs, is highly depending on the doping level of NEs. For comparison, rate-capability and cycle performance of the LIC with a doping level of 100% (17.2 wt% of $Li_6CoO_4$) were also examined under the same experimental conditions. More detailed information on cell configuration and doping profiles are given in Table S2 and Fig. S13, respectively. The LIC showed comparable rate capability and cycle performance with conventional LIC during cycles as shown in Fig. 6e and Fig. 6f, respectively. After 1000 cycles, the LIC with $Li_6CoO_4$ exhibited a capacity retention of 98.2 % and 98.0% for conventional LIC. Our approach also has the benefit of being able to increase volumetric energy density and assure the safety of the LIC by eliminating metallic Li from the cell (Fig. 7). We emphasize that our proposed $Li^+$ pre-doping method using $Li_6CoO_4$ is favourable for increasing the energy density and securing the safety of LICs without loss of significant electrochemical performance. Compared with other candidates, the $Li_6CoO_4$ also shows great promise as a promising alternative $Li^+$ source with distinct strengths of large available capacity (> 600 $mAhg^{-1}$ and low charging voltage (< 4.3 V *vs.* $Li/Li^+$). The technology would be helpful for developing advanced LICs and for making advances toward their commercial use.

## Conclusions

A highly irreversible characteristic of $Li_6CoO_4$ would be advantageous to its use as an alternative $Li^+$ source for an efficient $Li^+$ pre-doing process for LICs. It provides a large amount of available $Li^+$ (about 600 mAh $g^{-1}$) for pre-lithiation of the NE by electrochemical charging to 4.3 V vs. $Li/Li^+$. In practical applications, $Li^+$ pre-doping can be achieved with a smaller amount of $Li_6CoO_4$ and undesirable side reactions, associated with electrolyte decomposition at high operating voltages (over 4.3 V vs. $Li/Li^+$), can be prevented. In this work, the origin of the distinct electrochemical behaviour and the structural stability of $Li_6CoO_4$ were thoroughly investigated, based on electrochemical experiments and theoretical validations. Importantly, less than 3.5 mol of $Li^+$ in the $Li_6CoO_4$ is available for $Li^+$ pre-doping without significant structural collapse of the structure accompanied with $O_2$ evolution. Furthermore, the feasibility of $Li_6CoO_4$ as an alternative $Li^+$ source was examined in LIC applications. The highly irreversible behaviour of $Li_6CoO_4$ was beneficial for further improvement of energy density and safety of current LICs. We demonstrated advanced LIC by incorporation of $Li_6CoO_4$ into the positive electrode and removing auxiliary metallic Li from the cell.

## Acknowledgments

This work was supported by the IT R&D program (10046306, Development of Li-rich Cathode (≥240 mAh/g) and Carbon-free Anode Materials (≥1,000 mAh/g) for High Capacity/High Rate Lithium Secondary Batteries) of MOTIE/KEIT, Republic of Korea and the National Research Foundation of Korea (NRF) grant funded by MEST (2012R1A3A2048841), Republic of Korea.

## Notes and references

[a] *Advanced Batteries Research Centre, Korea Electronics Technology Institute, Seongnam, 463-816, Republic of Korea. Fax: +82-31-789-7499; Tel: +82-31-789-7496; E-mail: parkms@keti.re.kr*
[b] *School of Mechanical and Aerospace Engineering, Seoul National University, Seoul 151-742, Republic of Korea.*
[c] *Department of Materials Science and Engineering, University of Texas at Dallas, Richardson, TX75080, USA. E-mail: kjcho@utdallas.eud*
[d] *Department of Chemical Engineering, Dong-A University, Busan 604-714, Republic of Korea.*
[e] *Department of Materials Science and Engineering, Korea University, Seoul 136-701, Republic of Korea.*

† Electronic Supplementary Information (ESI) available: additional experimental data and equations for DFT calculations are included. See DOI: 10.1039/b000000x/

‡ First and second author contributed equally to this work.

1 R. Kotz and M. Carlen, *Electrochim. Acta*, 2000, **45**, 2483.
2 A. D. Pasquier, I. Plitz, S. Menocal and G. Amatucci, *J. Power Sources*, 2003, **115**, 171.
3 W. Li and G. Joos, *Proc. IEEE Power Electron. Specialists Conf.*, 2008, 1762.
4 M. E. Glavin, Paul K. W. Chan, S. Armstrong and W. G. Hurley, *Proc. IEEE Power Electron. Motion Control Conf.*, 2008, 1688.
5 S. Vazquez, S. M. Lukic, E. Galvan, L. G. Franquelo and J. M. Carrasco, *IEEE Trans. Industrial Electronics*, 2010, **57**, 3881.
6 J. Cao and A. Emadi, *IEEE Trans. Power Electronics*, 2012, **27**, 122.
7 T. M. Masaud, K. Lee and P. K. Sen, *Proc. IEEE North American Power Symposium*, 2010, 1.
8 I. Hadjipaschalis, A. Poullikkas and V. Efthimiou, *Renewable Sustainable Energy Rev.*, 2009, **13**, 1513.
9 C. Liu, F. Li, L.-P. Ma and H.-M. Cheng, *Adv. Mater.*, 2010, **22**, E28.
10 G. G. Amatucci, F. Badway, A. D. Pasquier and T. Zheng, *J. Electrochem. Soc.*, 2001, **148**, A930.
11 A. Yoshino, T. Tsubata, M. Shimoyamada, H. Satake, Y. Okano, S. Mori and S. Yata, *J. Electrochem. Soc.*, 2004, **151**, A2180.
12 K. Naoi and P. Simon, *Electrochem. Soc. Interf.*, 2008, **17**, 34.
13 K. Naoi, *Fuel cells*, 2010, **10**, 825.
14 R. B. Sepe, A. Steyerl and S. P. Bastien, Proc. *IEEE Energy Conversion Congress & Exposition*, 2011, 1813.
15 J. R. Miller and A. F. Burke, *Electrochem. Soc. Interf.*, 2008, **17**, 53.
16 A. K. Shukla, A. Banerjee, M. K. Ravikumar, and A. Jalajakshi, *Electrochim. Acta*, 2012, **84**, 165.
17 F. Ciccarelli and D. Iannuzzi, *Proc. Int. Symp. Power Electronics, Electrical Drives, Automation and Motion*, 2012, 773.
18 M.-S. Park, Y.-G. Lim, J.-H. Kim, Y.-J. Kim, J. Cho and J.-S. Kim, *Adv. Energy Mater.*, 2011, **1**, 1002.

19 M.-S. Park, Y.-G. Lim, S. M. Hwang, J. H. Kim, J.-S. Kim, S. X. Dou, J. Cho and Y.-J. Kim, *ChemSusChem*, 2014, (DOI 10.1002/cssc.201402397).
20 M.-S. Park, Y.-G. Lim, J.-W. Park, J.-S. Kim, J.-W. Lee, J. H. Kim, S. X. Dou and Y.-J. Kim, *J. Phys. Chem. C*, 2013, **117,** 11471.
21 M. M. Thackeray, Maria K. Y. Chan, L. Trahey, S. Kirklin and C. Wolverton, *J. Phys. Chem. Lett.*, 2013, **4**, 3607.
22 M. Noh and J. Cho, *J. Electrochem. Soc.*, 2012, **159**, A1329.
23 R. Luge and R. Hoppe, *Z. Anorg. Allg. Chem.*, 1986, **534**, 61.
24 M. K. Aydinol and G. Ceder, *J. Electrochem. Soc.*, 1997, **144**, 3832.
25 C. Frayret, A. Villesuzanne, N. Spaldin, E. Bousquet, J.-N. Chotard, N. Recham and J.-M. Tarascon, *Phys. Chem. Chem. Phys.*, 2010, **12**, 15512.
26 D. Carlier, A. Van der Ven, C. Delmas and G. Ceder, *Chem. Mater.*, 2003, **15**, 2651.
27 M. Wagemaker, A. Van Der Ven, D. Morgan, G. Ceder, F. M. Mulder and G. J. Kearley, *Chemical Physics*, 2005, **317**, 130.



 

**Graphical abstract**

A single phase $Li_6CoO_4$ with an anti-fluorite structure is proposed as a promising lithium source for high-energy lithium ion capacitors. By integration of $Li_6CoO_4$, energy density of lithium ion capacitor can be significantly improved. Electrochemical and structural stabilities of $Li_6CoO_4$ are thoroughly investigated based on first principles calculations and experimental validations.